Proceedings of GT2007
ASME Turbo Expo 2007: Power for Land, Sea and Air
May 14-17, 2007, Montreal, Canada

GT2007-27996

TURBINE AIRFOIL NET HEAT FLUX REDUCTION WITH CYLINDRICAL HOLES EMBEDDED IN A TRANSVERSE TRENCH

Katharine L. Harrison, John R. Dorrington, Jason E. Dees, and David G. Bogard
University of Texas at Austin, Mechanical Engineering Department, Austin, TX, USA

Ronald S. Bunker
GE Global Research Center, Niskayuna, NY, USA

ABSRACT

Film cooling adiabatic effectiveness and heat transfer coefficients for cylindrical holes embedded in a 1*d* transverse trench on the suction side of a simulated turbine vane were investigated to determine the net heat flux reduction. For reference, measurements were also conducted with standard inclined, cylindrical holes. Heat transfer coefficients were determined with and without upstream heating to isolate the hydrodynamic effects of the trench and to investigate the effects of the thermal approach boundary layer. Also the effects of a tripped versus an un-tripped boundary layer were explored. For both the cylindrical holes and the trench, heat transfer augmentation was much greater with no tripping of the approach flow. A further increase in heat transfer augmentation was caused by use of upstream heating, with as much as a 150% augmentation with the trench. With a tripped approach flow the heat transfer augmentation was much less. The net heat flux reduction for the trench was found to be significantly higher than for the row of cylindrical holes.

INTRODUCTION

Today's modern gas turbines are subjected to extremely high temperatures and thermal stresses during normal operation. The thermal conditions that turbine components are exposed to actually exceed the materials limits of the components. Cooling techniques must therefore be utilized to prevent failure and provide satisfactory component life.

Recently, studies by Bunker [1], Waye and Bogard [2], Lu et al. [3], and Dorrington and Bogard [4] conducted on cylindrical holes embedded in transverse trenches showed significant improvements in adiabatic effectiveness over standard inclined, cylindrical holes. Bunker [1] studied the effects of axial and radial holes embedded in a transverse trench with depths s/d = 0.43 and s/d = 3, respectively. This study showed that the centerline adiabatic effectiveness improved by 50% to 75% in the region of x/d < 40 for the axial holes. Waye and Bogard [2] studied various upstream and downstream trench lip configurations with a constant trench depth of s = 0.5d. They determined that the best performing configurations were those with a sharp rectangular trench lip immediately downstream of the coolant hole exit. Another important finding of [2] was that the trench suppressed jet separation and increased lateral coolant spreading. Lu et al. [3] studied the adiabatic effectiveness of five trench configurations with a uniform trench depth of 0.4d. One of their best configurations also had a sharp rectangular downstream trench lip.

More recently, Dorrington and Bogard [4] tested many trench configurations and determined that a 0.75d depth trench produced 40% greater average adiabatic effectiveness levels than a 0.5d depth trench, and a 1.0d trench performed similarly to the 0.75d trench. Furthermore, they found that the adiabatic effectiveness for the best trench configuration was similar to that for a row of shaped holes. This is important because the trench may prove to be significantly cheaper to manufacture than shaped holes.

In addition to determining adiabatic effectiveness, it is important to examine heat transfer coefficient augmentation, since increased mixing from injection can increase the heat transfer rate. Several heat transfer studies have been conducted on film cooled surfaces to determine heat transfer coefficient augmentation. Ericksen and Goldstein [5], Baldauf et al. [6], and Ammari et al. [7] measured augmentation that was less than 10% for a blowing ratio of M = 0.5, except within the first few hole diameters downstream of the hole.

Most studies in open literature do not heat the surface upstream of the film cooling holes. It is generally assumed that upstream heating has a small effect on heat transfer coefficient augmentation. A few studies have examined the effects of an upstream thermal boundary layer. Mayhew et al. [8] measured heat transfer coefficient augmentation using upstream heating and, for M = 0.5, found augmentation from

15% to 5% which the authors claimed was higher than for previous studies with unheated starting length. The study attributed the elevated augmentation to the use of upstream heating. Kelly and Bogard [9] showed increased augmentation near the holes on a flat plate when upstream heating was used, but the effect subsided downstream. Coulthard et al. [10] found that the heat transfer coefficient augmentation was not significantly affected by upstream heating at high blowing ratios, but at low blowing ratios there was an increased augmentation, especially near the holes.

Heated and unheated starting lengths are both useful for fully characterizing heat transfer coefficient augmentation. With an unheated starting length, i.e. with downstream heating alone, changes in the heat transfer coefficient are due to hydrodynamic effects alone because there is no upstream thermal boundary layer. However, since the actual airfoil will generally have heating (or cooling) of the flow upstream of the coolant holes, upstream heating is a more realistic simulation. In this study, heat transfer coefficient augmentation was examined for both heated and unheated starting length configurations.

Since it is possible to negate the benefits of film cooling if heat transfer coefficients are increased significantly by the injection process, the net effect on heat transfer rate to the surface is commonly estimated using the net heat flux reduction, Δq_r. This parameter is a measure of how much film cooling reduces the heat flux to the wall relative to the heat flux that would occur with no film cooling. The adiabatic effectiveness and heat transfer coefficients are combined to determine the net heat flux reduction, Δq_r, using the following equation (derivation shown in [11]):

$$\Delta q_r = 1 - \frac{h_f}{h_0}\left(1 - \frac{\eta}{\phi}\right) \quad (1)$$

The ϕ parameter in this equation, referred to as the overall effectiveness, is the normalized surface temperature for the actual airfoil. Generally the overall effectiveness is assumed to be $\phi = 0.6$ for calculation of the net heat flux reduction, and $\phi = 0.6$ was assumed for this study.

The primary goal of this study was to determine the heat transfer coefficient augmentation caused by coolant injection through a 1*d* deep, 2*d* wide trench, and ultimately the net heat flux reduction that can be achieved with this trench. For reference, measurements were also made using a baseline case consisting of a row of cylindrical, inclined holes. Since the approach boundary layer was transitional without a trip, measurements were done with and without an upstream trip to induce a turbulent boundary layer. Baseline adiabatic effectiveness data from Waye and Bogard [2] and trench adiabatic effectiveness data from Dorrington and Bogard [4] were used to calculate the net heat flux reduction. The trench technology tested in this study is described in the US patent 6,234,755.

NOMENCLATURE

c = Chord length
d = Hole diameter
DR = Density ratio = ρ_c/ρ_∞
h_0 = Heat transfer coefficient without film cooling = $q"/(T_\infty - T_{surf})$
h_f = Heat transfer coefficient with film cooling = $q"/(T_\infty - T_{surf})$
h_f/h_0 = Heat transfer coefficient augmentation
I = Current
k = Thermal conductivity
l = Hole length
L = Thickness of airfoil wall
M = Blowing ratio = $\rho_c U_c/\rho_\infty U_\infty$
p = Hole spacing
$q"$ = Heat flux
Δq_r = Net heat flux reduction
Re = Reynolds number
s = Trench depth
T = Temperature
Tu = Mainstream turbulence intensity
U = Velocity
V = Voltage
w = Trench width
X = Streamwise coordinate originating at the stagnation line
x = Streamwise coordinate originating at downstream edge of the trench insert
y = Coordinate normal to the vane surface
z = Spanwise coordinate

Greek

Λ = Mainstream turbulence length scale
α = Injection angle
δ = Boundary layer thickness
ε = Emissivity
ϕ = Overall effectiveness = $(T_{surf}-T_\infty)/(T_{c,i}-T_\infty)$
η = Adiabatic effectiveness = $(T_{aw}-T_\infty)/(T_{c,exit}-T_\infty)$
η_0 = Conduction error
ρ = Density
σ = Stephan-Boltzmann constant

Subscripts and Superscripts

$-$ = Laterally Averaged
∞ = Mainstream
aw = Adiabatic wall
c = Coolant
$exit$ = Evaluated at hole exit
i = Evaluated internally in the plenum
$surf$ = Wall surface

FACILITIES AND PROCEDURES

All experiments were conducted in a closed loop wind tunnel driven by a 50 hp variable speed fan with adjustable pitch. The test section was a simulated three vane cascade schematically shown in Figure 1. The tests were conducted on the center vane, a 9x scaled up version of an actual turbine vane, as shown in Figure 2. The outer walls of the test section were carefully adjusted to match the non-dimensional pressure distribution around the vane based on an inviscid CFD simulation of the cascade flow. The Reynold's number was matched to real engine conditions. A turbulence generator was located at the entrance of the test section. It was

positioned 0.50 m upstream of the vane cascade and comprised of 12 vertical rods with diameter of 38 mm and spaced 85 mm apart. The mainstream turbulence was previously measured by Robertson [12] to be 21% with an integral length scale of Λ/d = 10.0.

The vane was manufactured from polyurethane foam with k = 0.048 W/m·K. A removable section of the vane, made of the same material, was used to vary configurations and test the trench and baseline row of holes. The trench was milled in the removable section which had a row of 18 coolant holes. For the baseline configuration, the trench was filled with an insert with cylindrical holes. The trench was 2d wide with the vertical trench lips being positioned flush with the upstream and downstream exits of the hole as shown in Figure 3. This trench configuration was the most effective of 15 different trench configurations tested in the companion study [4]. Only one row of holes was examined in this study as shown in Figure 2, and all other rows of holes were sealed off. Pertinent geometrical and flow parameters are presented in Table 1.

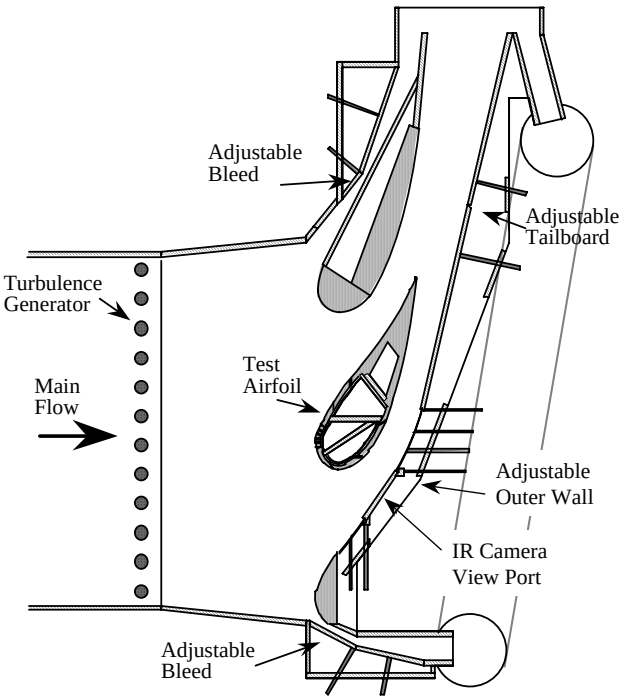

Fig. 1 Schematic of test section

The adiabatic effectiveness, η, is a measure of how well the surface of the airfoil is being cooled. It is defined as follows:

$$\eta = \frac{T_{aw} - T_{\infty}}{T_{c,exit} - T_{\infty}} \qquad (2)$$

The surface temperature, T_{aw}, used for the adiabatic effectiveness was measured using a FLIR ThermaCAM P20 infrared camera. The camera was calibrated using ribbon E-type thermocouples located on the surface. The thermocouple data was acquired by a National Instruments Data Acquisition system.

The adiabatic effectiveness experiments were conducted using a coolant to mainstream density ratio of 1.3. This was achieved by using liquid nitrogen to cool the air before entering the vane plenum. There were three different independent plenums in the vane, but all tests conducted in this study were done on the suction side, and no coolant was allowed to enter the pressure side or showerhead plenums. The coolant air was bled off of the mainstream flow at a location just upstream of the wind tunnel fan. The air was then pumped into a heat exchanger where it was cooled by liquid nitrogen prior to entering the vane suction side plenum.

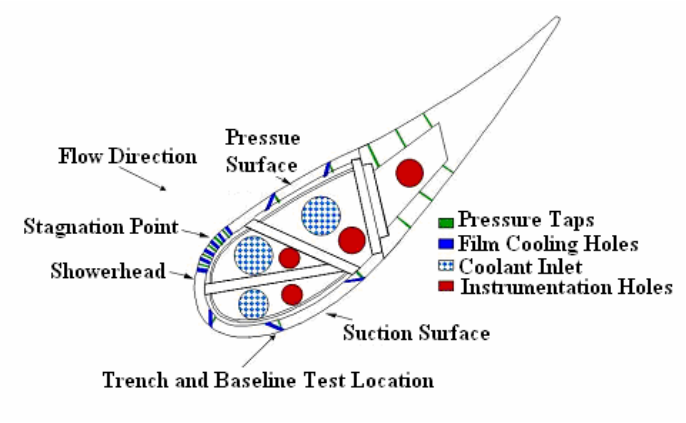

Fig. 2 Detailed representation of the test vane

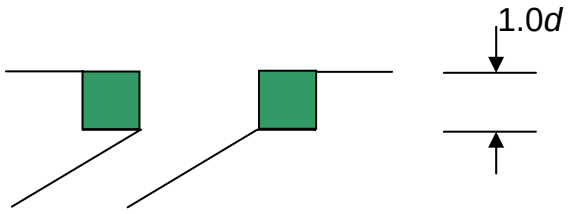

Fig. 3 Narrow trench configuration

Due to the finite thermal conductivity of the polyurethane test section, a one dimensional conduction correction was employed when processing the adiabatic effectiveness data. The appropriate conduction correction was determined using measurements of the surface temperature with the exit of the coolant holes blocked to directly determine the conduction error. This conduction error, denoted η_o, was used to establish the conduction correction for the adiabatic effectiveness as follows:

$$\eta = \frac{\eta_{measured} - \eta_0}{1 - \eta_0} \qquad (3)$$

The conduction correction was found to be η_0 = 0.040 ± 0.015. More details on adiabatic effectiveness tests are available in [2] and [4].

Heat transfer experiments were run by securing 0.38 mm thick type 302 stainless steel heat flux foils to the surface of the vane upstream and downstream of the trench. The heat flux foils were attached to the surface directly upstream and downstream of the inserts. The heat flux foils were covered

with a layer of flat black vinyl cardstock to smooth steps before and after the plates. This also provided a smooth wall and repeatable surface conditions. Heat flux experiments were conducted using a 1*d* depth trench. Both heat flux plates were attached to the surface regardless of whether upstream heating was used so that the hydrodynamic approach conditions were the same with and without upstream heating. All heat transfer experiments were conducted using a density ratio of *DR* = 1.0 to reduce measurement uncertainties.

Table 1 Test condition data

Hole Diameter	d = 4.11 mm
Pitch	$p = 2.775d$
Trench Depth	$s = 1d$
Trench Width	$w = 2d$
Hole Angle	$\alpha = 30^o$
Hole Length (without trench)	$l = 6.7d$
Hole Length (with trench)	$l = 4.7d$
Mainstream Temperature	T = 300 K
Mainstream Velocity (at tunnel inlet)	U_∞ = 5.8 m/s
Mainstream Re (based on the chord length at the tunnel inlet)	$Re = 2.2x10^5$
Mainstream Turbulence (at tunnel inlet)	Tu = 21%
Mainstream Turbulence Length Scale	Λ/d = 10
Chord Length	c = 59.4 cm
Vane Span	54.9 cm
Vane Pitch	45.7 cm
Position of Trench	X/c = 0.367
Position of Trip	X/c = 0.285

The FLIR IR camera was used to record surface temperatures and was calibrated using two type E thermocouples on the surface of the vane. To produce a uniform heat flux, electrical current from a power supply was supplied to the heat flux foils. The voltage across a shunt resister was used to determine the current, and the voltage drop was measured across the downstream heat flux plate. The heat flux through the surface was found by the following equation, in which *A* is the area of the downstream heat flux plate:

$$q''_{generated} = \frac{IV}{A} \tag{4}$$

A thermocouple was attached to the interior surface of the vane to determine the internal temperature, T_i, such that conduction corrections could be determined. The convective heat flux supplied to the surface was found by subtracting the losses due to conduction and radiation, as follows:

$$\begin{aligned} q''_{convection} &= q''_{generated} - q''_{conduction} - q''_{radiation} \\ &= q''_{generated} - \frac{k}{L}(T_{surf} - T_i) - \varepsilon\sigma(T^4_{surf} - T^4_\infty) \end{aligned} \tag{5}$$

The conduction and radiation corrections typically accounted for approximately 4% and 6% of the total heat flux, respectively.

The heat flux foils were attached in series so the current through the upstream and downstream heat flux foils was equal. The upstream heat flux plate spanned 21.7*d* upstream of the upstream edge of the trench insert and the downstream heat flux plate spanned 27.0*d* downstream of the downstream edge of the insert, resulting in 25% greater heat flux upstream than downstream. This higher heat flux for the upstream foil was used because the upstream heat flux did not span all the way from the stagnation line. However, the 25% higher heat flux was arbitrary and represents only one of many possible upstream heating conditions.

Heat transfer coefficients without film cooling, h_0, were measured by filling the trench with an insert and covering the entire surface up to the stagnation line with cardstock. An insert with extensions of the cylindrical, inclined holes was used to test the baseline configuration. For the tripped configurations, a 0.4 mm diameter trip was positioned at X/c = 0.285 as shown in Figure 4. One hole diameter upstream of the trench, the boundary layer thicknesses with and without the trip were measured to be δ = 3.2 mm and 1.2 mm, respectively. The tripped boundary profile was very close to a 1/7th power law correlation, and the un-tripped profile was transitional, as shown in Figure 5.

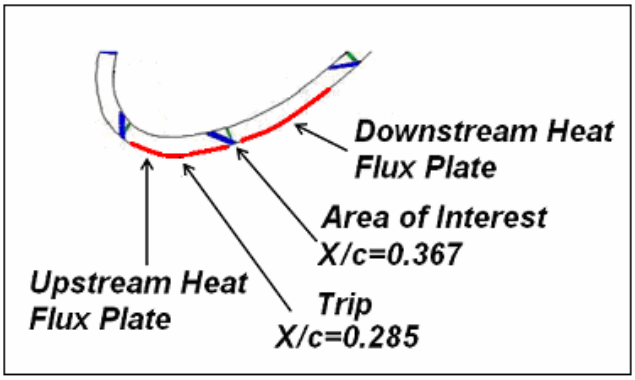

Fig. 4 Location of trip and heat flux plates

The baseline adiabatic effectiveness measurements used to calculate the net heat flux reduction were taken from Waye and Bogard [2]. Through analysis of data from [2], the boundary layer thickness was found to be 1.5 mm. The trench adiabatic effectiveness measurements were taken from Dorrington and Bogard [4]. The boundary layer thickness was not measured but the approach conditions were similar to the un-tripped heat transfer tests.

Uncertainty in the measurements was calculated using the sequential perturbation method described by Moffat [13]. The uncertainty in adiabatic effectiveness was found to be $\delta\overline{\eta}$ = ± 0.02 or less for all measurements by both sequential perturbation and test-to-test repeatability measurements. The following uncertainties were included in the analysis: the IR camera calibration, thermocouple measurements, the blowing ratio, and the conduction correction. See [2] and [4] for more information on the adiabatic effectiveness measurements.

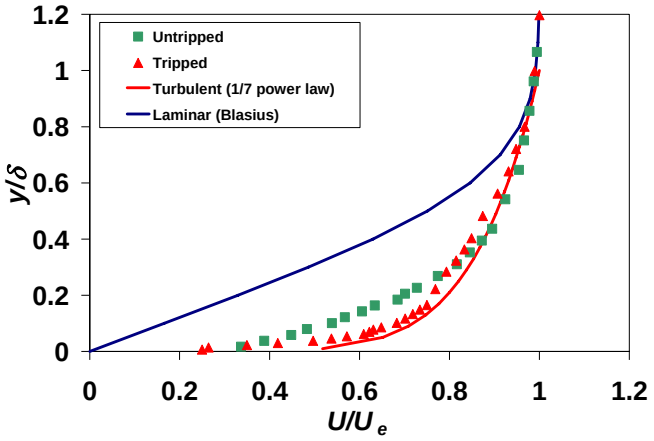

Fig. 5 Boundary layer profiles for tripped and untripped heat transfer experiments

Using sequential perturbation, the average uncertainty in heat transfer measurements with film cooling was found to be δh_f = 5.7%, and the average uncertainty in heat transfer measurements without film cooling was found to be δh_0 = 5.0%. The average uncertainty in heat transfer augmentation values was calculated to be $\delta(h_f/h_0)$ = 7.8% and the average uncertainty in net heat flux reduction calculation was $\overline{\delta \Delta q_r}$ = ±0.06. All uncertainty values are determined at a 95% confidence level. Uncertainty calculations for heat transfer testing included: the IR camera calibration, thermocouples, the conduction correction, the radiation correction, and the uncertainties in the current and voltage measurements. The largest source of uncertainty was the uncertainty for surface temperature measurements with the IR camera which was ±0.5 K. Bias errors due to conduction into the airfoil wall, 4%, and radiation to surroundings, 6%, were corrected as discussed previously. Repeatability of measurements within a test was checked in every experiment. In-test repeatability for the h_f and h_0 measurements was found to be ±2-4%. The h_0 configurations were repeated in multiple tests, and the test-to-test repeatability was found to be ±5%.

RESULTS

To fully characterize film cooling performance, it is necessary to measure both the adiabatic effectiveness and heat transfer coefficient augmentation. Adiabatic effectiveness downstream of the narrow trench is compared to that for a baseline row of cylindrical holes in Figure 6. These results were taken from [2] and [4], and are presented in terms of laterally averaged effectiveness, $\overline{\eta}$, for blowing ratios of M = 0.6, 1.0, and 1.4. The trench exhibited increasing $\overline{\eta}$ levels with increasing blowing ratio, while $\overline{\eta}$ levels for the cylindrical holes decreased with increasing M. At the lowest blowing ratio shown of M = 0.6, the performance for the cylindrical holes and the trench were comparable. However, at blowing ratios of M = 1.0 and 1.4, for which cylindrical hole performance dropped dramatically because of jet separation, the trench performance continued to increase substantially. Ultimately for M = 1.4, $\overline{\eta}$ levels for the trench were more than three times greater than that for baseline cylindrical holes. Refer to [2] and [4] for more details.

To illustrate the differences between the trench and baseline configurations, Figure 7 presents contour plots of adiabatic effectiveness for M = 1. The trench increased lateral coolant spreading and greatly increased adiabatic effectiveness. For the baseline cylindrical hole configuration, streaks of higher η are evident at the location of distinct coolant jets. The individual jets are much less visible on the contour plot for the trench configuration. Refer to [2] and [4] for more explanation on how the trench increased adiabatic effectiveness.

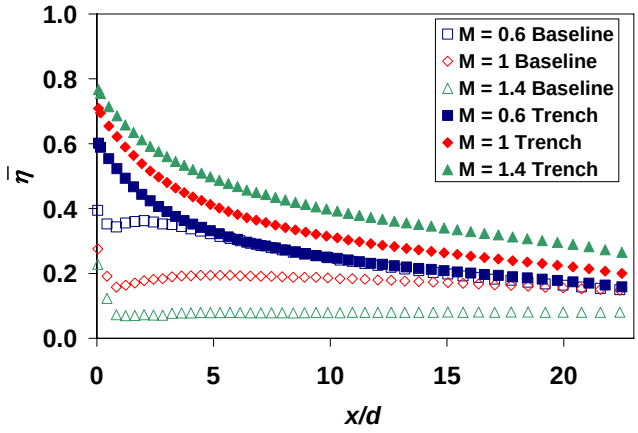

Fig. 6 Distributions of $\overline{\eta}$ for the baseline and trench without a trip

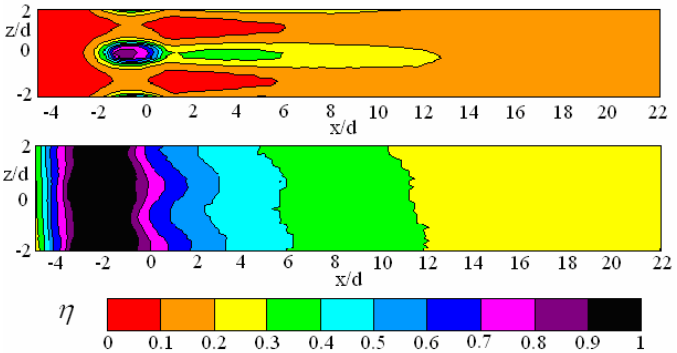

Fig. 7 Adiabatic effectiveness surface contours without upstream heating and without a trip for the baseline (top) and trench (bottom)

Examination of heat transfer coefficients is important because injection of coolant can lead to heat transfer coefficient augmentation. Heat transfer coefficient augmentation measurements are presented for four different configurations: heated and unheated starting lengths, and tripped and un-tripped approach boundary layers. An unheated starting length was used to isolate the hydrodynamic effects. This allowed the hydrodynamic boundary layer effects to be analyzed without being influenced by an upstream thermal boundary layer. Unheated starting length measurements are also useful because net heat flux reduction

is commonly presented in literature for this configuration. Heated starting length measurements were taken to illustrate the effect of a heated upstream thermal boundary layer since operational airfoils are heated upstream.

There are two reasons for tripping the flow. First, rough surface conditions on operational airfoils and leading edge showerhead blowing would probably cause transition to turbulence on an actual airfoil. Second, a comparison between the tripped and un-tripped heat transfer coefficients with blowing to tripped and un-tripped $\overline{h_0}$ values allowed determination of whether blowing increased augmentation by essentially causing transition to turbulence. Baseline heat transfer coefficient augmentation was also measured for comparison to the trench.

Heat transfer coefficient augmentation contour plots of the untripped baseline and trench configurations for M = 1 without upstream heating are shown in Figure 8. Unlike the adiabatic effectiveness contour plots shown in Figure 7, individual jets were not visible in the heat transfer coefficient augmentation contours. The contour plots demonstrate that augmentation was fairly uniform laterally. For the following results, only laterally averaged heat transfer coefficient augmentation will be discussed.

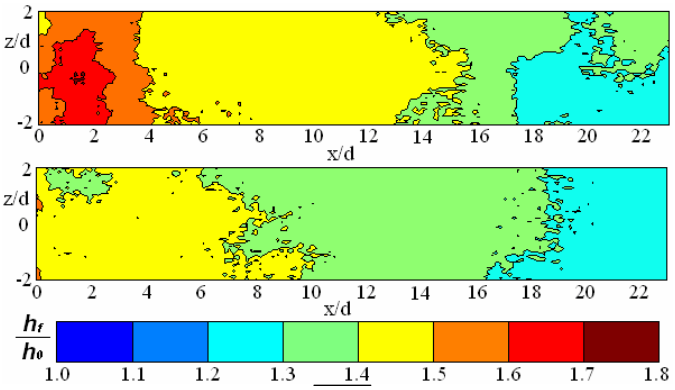

Fig. 8 Surface contours of $\overline{h_f / h_0}$ without upstream heating and without a trip for the baseline (top) and the trench (bottom)

For reference the heat transfer coefficients, $\overline{h_0}$, for an airfoil surface with no film cooling holes or a trench were measured. These reference cases are presented in Figure 9 for all four heat transfer configurations, i.e. with and without upstream heating, and with and without a boundary layer trip. As expected, an unheated starting length resulted in much higher $\overline{h_0}$ initially because of the development of a new thermal boundary layer. Also, $\overline{h_0}$ values for the unheated starting length decayed faster than $\overline{h_0}$ for the heated starting length, such that the difference between the two values reduced with downstream distance. In theory, given sufficient development length, unheated starting length $\overline{h_0}$ values will become equivalent to those for the heated starting length. However, this did not occur over the distance of x/d = 23 measured in these experiments.

Also evident in Figure 9 are much lower $\overline{h_0}$ values for the cases without a boundary layer trip. With upstream heating, the trip caused 40% to 60% increases in $\overline{h_0}$. This can be attributed to the trip causing the transitional boundary layer to become fully turbulent as noted earlier. Without upstream heating, tripping the flow caused a 10% to 20% increase in $\overline{h_0}$.

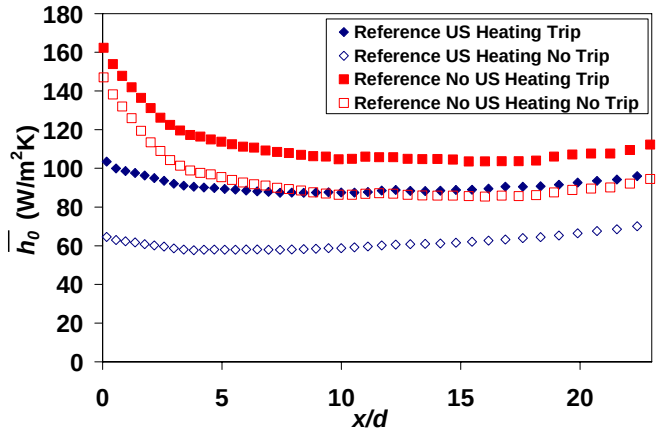

Fig. 9 Reference smooth surface $\overline{h_0}$ values for four operating conditions

Before presenting results of the effects of the shallow trench on enhancing heat transfer coefficients, it is informative to examine the effects of film injection from the baseline cylindrical hole configuration. Figure 10 shows laterally averaged heat transfer coefficient augmentation, $\overline{h_f / h_0}$, for the baseline with heated and unheated starting lengths and without a trip. Results for three blowing ratios, M = 0.6, 1.0, and 1.4, are presented, and a condition designated M = 0 which indicates measurements with the holes exposed but with no blowing. Immediately obvious from this figure is a significantly higher augmentation, $\overline{h_f / h_0} \approx 2$, with upstream heating compared to $\overline{h_f / h_0} \approx 1.5$ without upstream heating. This significant increase in the heat transfer coefficient can be attributed to the effect of the coolant jets displacing the upstream thermal boundary layer. Even for the unheated starting length condition, the coolant jets caused a 50% enhancement in the heat transfer coefficient. In this case the increase is due to hydrodynamic effects, and is likely due to the jets promoting transition of the boundary layer flow to fully turbulent flow.

Augmentation of the heat transfer coefficients for the baseline row of holes with and without upstream heating and with a tripped approach flow is shown in Figure 11. With no upstream heating the augmentation was at most 15%, significantly less than the no trip case. This can be attributed to the trip causing transition of the boundary layer to fully turbulent flow so that the coolant jet injection had little additional impact on the flow. The case with upstream heating had a maximum augmentation of 30%, i.e. slightly larger than the unheated starting length case. Consequently the displacement of the upstream thermal boundary layer did cause an additional increase in heat transfer coefficient, but the increase was smaller than that for an untripped approach flow.

Measurements of heat transfer coefficient augmentation for the trench showed trends similar to the baseline case. Values of $\overline{h_f / h_0}$ for the trench with and without upstream heating and with no boundary layer trip are presented in Figure 12. Data are presented for blowing ratios of M = 0, 0.6, 1.0, 1.4, and 1.8. Augmentation values without upstream heating were as high as 50% near the hole and were still 25% by 20d downstream. Enhanced $\overline{h_f / h_0}$ in this case was due to the hydrodynamic effects of the trench since this configuration lacked an upstream thermal boundary layer. Coolant injection through the trench caused the boundary layer to transition to turbulent. With upstream heating, there was as much as 150% augmentation close to the trench, with still a 50% augmentation by 20d downstream. Enhancement over the unheated starting length case was due to displacement of the upstream thermal boundary layer. Similar to the baseline row of holes, $\overline{h_f / h_0}$ was increased considerably by the presence of upstream heating.

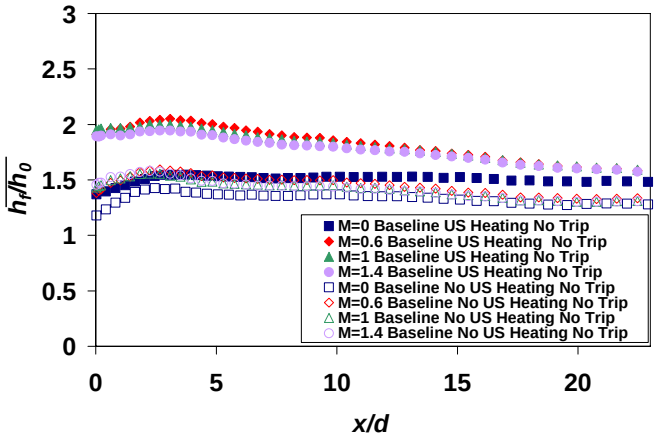

Fig. 10 Baseline $\overline{h_f / h_0}$ with and without upstream heating and without a trip

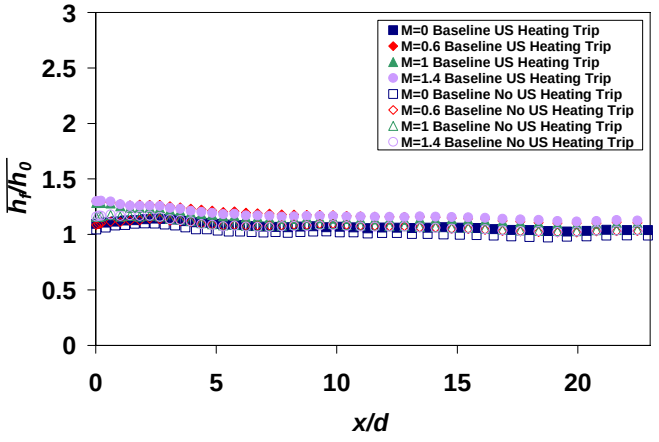

Fig. 11 Baseline $\overline{h_f / h_0}$ with and without upstream heating and with a trip

Augmentations of heat transfer coefficients with and without upstream heating, and with a tripped approach flow, are presented in Figure 13 for the trench. With an unheated starting length, augmentation was only 6% by 10d downstream, but augmentation was 20% with upstream heating at the same location. Close to the trench the augmentation was as much as 70%. Augmentation for the tripped approach boundary layer flow was much less than for the corresponding untripped cases. Without upstream heating, the M = 0 (no blowing) data showed no augmentation because the flow was already fully turbulent due to the trip and the trench could not further stimulate transition. The higher blowing ratios showed augmented $\overline{h_f / h_0}$ values relative to the M = 0 case, which can be attributed to interaction of the coolant flow with the mainstream.

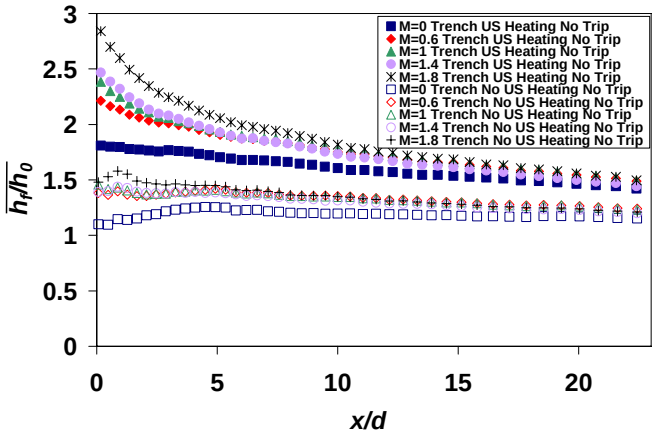

Fig. 12 Trench $\overline{h_f / h_0}$ with and without upstream heating and without a trip

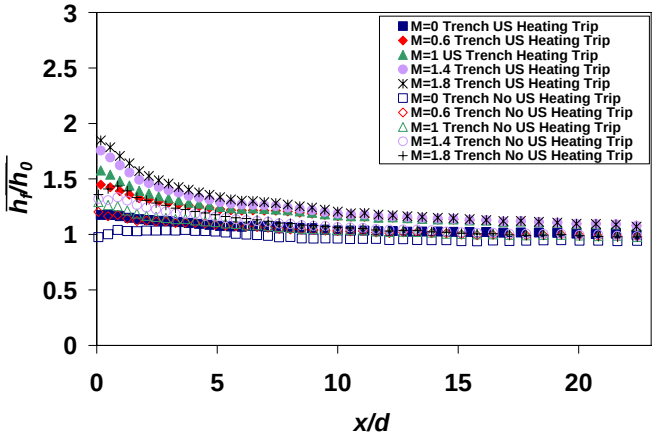

Fig. 13 Trench $\overline{h_f / h_0}$ with and without upstream heating with a trip

Because the $\overline{h_f / h_0}$ ratio varies with changes in either h_f or h_0, further insight can be gained by examining $\bar{h}_f$ alone for all four trench heat transfer configurations at M = 0 as shown in Figure 14. Immediately evident from the figure is that the $\bar{h}_f$ distributions were exactly the same for the tripped and untripped approach flows, for the same thermal approach conditions. This demonstrated that the trench effect on the boundary layer flow dominated to the extent that the approach flow was irrelevant. However, if the flow was already

turbulent, the presence of the trench did not cause a further increase in $\overline{h}_f$.

The heat transfer coefficient augmentation due to injection from a trench is compared to the baseline configuration in Figure 15. This figure shows baseline and trench $\overline{h_f/h_0}$ values at a blowing ratio of M = 1 for all four heat transfer testing configurations: tripped and untripped with and without upstream heating. As is clear from the figure, $\overline{h_f/h_0}$ values were very similar for the baseline and trench configurations, for all operating conditions.

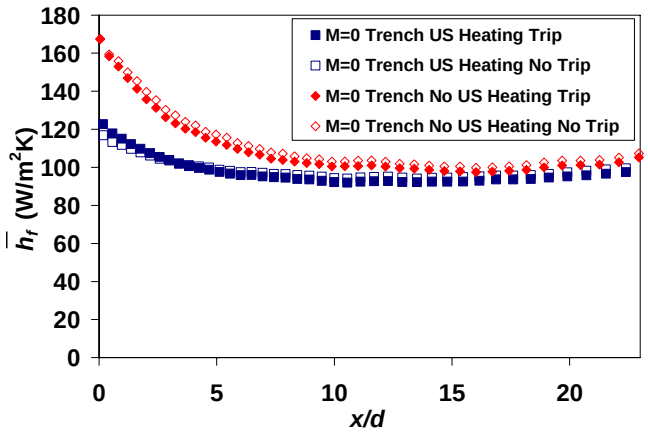

Fig. 14 Distributions of $\overline{h}_f$ with an exposed trench but with no blowing (M = 0)

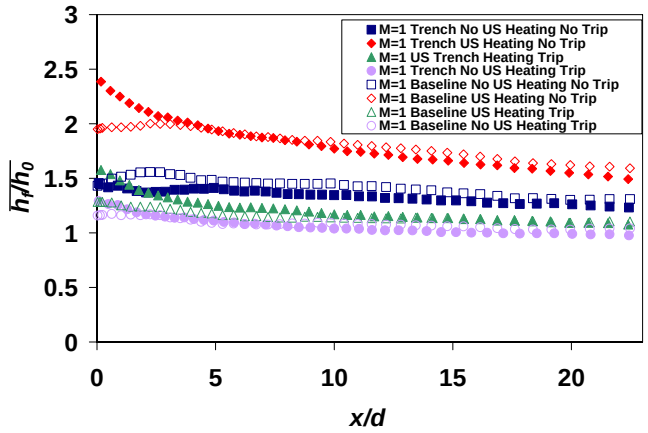

Fig. 15 Comparison of $\overline{h_f/h_0}$ for the trench and baseline at M = 1

To determine the balance between the beneficial effects of lowered temperature due to film cooling injection and the detrimental effects of augmented heat transfer coefficients, the net heat flux reduction, $\overline{\Delta q_r}$, was calculated. Since adiabatic effectiveness data with a trip was unavailable in [2] and [4], $\overline{\Delta q_r}$ was only calculated for the corresponding untripped heat transfer configurations.

The net heat flux reduction for the untripped baseline configuration with and without upstream heating is presented in Figure 16. The most striking results are the negative $\overline{\Delta q_r}$ values, which indicate that film cooling injection had a detrimental effect and could increase the net heat flux into the surface. The largest degradation in performance occurred at high blowing ratios, which can be attributed to the low $\overline{\eta}$ levels at high M. Also contributing to the low net heat flux reduction levels were the high $\overline{h_f/h_0}$ levels present for the untripped configurations. The lower $\overline{\Delta q_r}$ values for the upstream heated case can be attributed to larger $\overline{h_f/h_0}$ values with upstream heating than without.

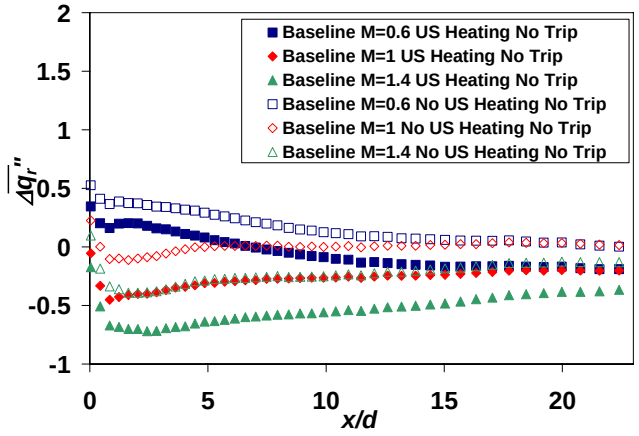

Fig. 16 Baseline $\overline{\Delta q_r}$ with and without upstream heating and without a trip

Values for $\overline{\Delta q_r}$ obtained using a trench were distinctly higher than the baseline results. Figure 17 shows the trench net heat flux reduction results, from which it is immediately obvious that $\overline{\Delta q_r}$ was essentially positive for all blowing ratios. The higher net heat flux reduction values were due to much higher $\overline{\eta}$ levels for the trench. In converse to the baseline case, $\overline{\Delta q_r}$ for the trench increased with blowing ratio due to increasing $\overline{\eta}$ levels with increasing blowing ratio. The performance with and without upstream heating were similar, especially at high blowing ratios with high $\overline{\eta}$ levels. Despite the large differences in $\overline{h_f/h_0}$ for the heated and unheated approach conditions, the very high $\overline{\eta}$ levels dominated over the effects of $\overline{h_f/h_0}$ and the net heat flux reduction remained high.

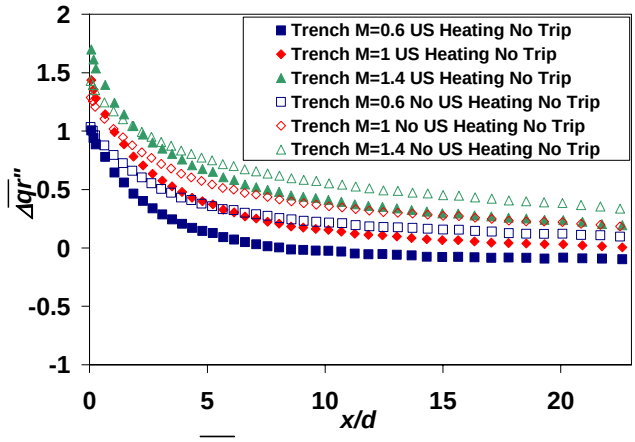

Fig. 17 Trench $\overline{\Delta q_r}$ with and without upstream heating without a trip

Of the two untripped configurations, the heated starting length is more representative of actual airfoils. Figure 18 shows $\overline{\Delta q_r}$ for the baseline and trench configurations with a heated starting length and an untripped boundary approach flow. At M = 0.6, baseline results after x/d = 5 were only slightly lower than the trench configuration due to similar $\overline{\eta}$ levels. At M = 1 and M = 1.4, $\overline{\Delta q_r}$ levels for the trench were much higher than the baseline, indicating the trench was much better at reducing heat flux into the surface.

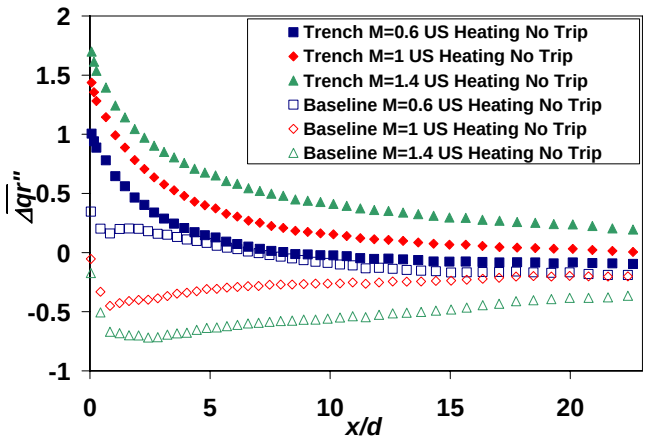

Fig. 18 Comparison of baseline and trench $\overline{\Delta q_r}$ levels with upstream heating and without a trip

CONCLUSIONS

This study examined the adiabatic effectiveness, heat transfer coefficients, and net heat flux reduction for film cooling with inclined cylindrical holes and with holes buried within a shallow trench. Experiments were done using a wind tunnel facility incorporating a simulated vane using a single row of holes located on the suction side of the vane. This study complements a companion study which showed significantly increased adiabatic effectiveness when coolant is injected into a shallow trench transverse to the flow.

To fully characterize heat transfer coefficient augmentation, $\overline{h_f / h_0}$; four reference operating conditions were examined: tripped and un-tripped boundary layer approach flows, each with heated and un-heated starting lengths. It was important to examine both heated and unheated starting lengths because upstream heating is more representative of actual airfoil conditions, but unheated starting length measurements are useful since they isolate the hydrodynamic effects of the trench. The four reference conditions resulted in four distinctly different distributions of heat transfer coefficients for the reference "no-holes" case, i.e. h_0. The h_0 distribution with no boundary layer trip was significantly lower, nominally 50%, than with a trip. Velocity profile measurements showed that this was due to a transitional boundary layer flow for the no-trip case, and a fully turbulent boundary layer for the tripped case. As expected, the unheated starting lengths resulted in higher h_0 distributions due to the delayed development of a thermal boundary layer.

The heat transfer augmentation obtained with inclined, cylindrical holes proved to be very dependent on the operating condition used. With no upstream trip, a significant augmentation occurred, 50% to 100%, which was attributed to the coolant hole (with no injection) or the coolant injection accelerating boundary layer transition. This was confirmed by the observation that with an upstream trip, there was negligible augmentation of the heat transfer coefficient when using no upstream heating. There was a significant difference in heat transfer augmentation when comparing heated and unheated upstream flow with no trip. The augmentation with a heated upstream flow was double that for an unheated upstream flow, i.e. 100% augmentation compared to 50% augmentation. This only occurred with coolant injection. The large increase in augmentation was attributed to the displacement of the upstream thermal boundary layer by the injected coolant. With an upstream trip, there was an increased augmentation when using a heated upstream flow, but the maximum augmentation was 30% near the hole, decaying to less than 15% by 20d downstream, i.e. much less than with an untripped flow.

The heat transfer augmentations that were found with coolant injection from holes embedded in a shallow trench were very similar to that found for the standard inclined hole configuration. The main difference was an increased augmentation near the coolant injection point for the trench when using a heated approach flow.

The overall performance of the film cooling configurations was evaluated by estimating the net heat flux reduction using measurements of adiabatic effectiveness and heat transfer coefficient augmentation. Since the heat transfer coefficient augmentation for the trench and baseline were similar, but the adiabatic effectiveness was much higher for the trench, the net heat flux reduction for the trench was much higher than the baseline. The average heat flux reduction for the trench configuration at high blowing ratios was greater than 50%, while the average heat flux reduction for standard holes at the optimum lower blowing ratio was less than 10%. The baseline configuration produced negative net heat flux reductions (i.e. the coolant injection caused an increase in heat transfer to the surface) for the higher blowing ratios, and even for lower blowing ratios for the no trip, heated upstream case. These negative net heat flux reduction values can be attributed to the large heat transfer augmentation that occurred for the no trip case. For the no trip case the reference heat transfer coefficient was much lower because the boundary layer was transitional and not fully turbulent. The coolant injection process caused a transition to fully turbulent flow, resulting in a large increase in the heat transfer coefficient. Consequently, for higher blowing ratio where the adiabatic effectiveness was poor, the large augmentation of the heat transfer coefficient caused an increase in the overall heat transfer to the wall. Although the trench configuration had similar, if not greater augmentation of the heat transfer coefficients than the standard hole configuration, the net heat flux reduction was significantly higher because of the much larger adiabatic effectiveness produced by the trench.

ACKNOWLEDGEMENTS

The authors gratefully acknowledge the Office of Naval Research (ONR) and the General Electric Corporation for their support of this research. A special thanks also goes to Brian Mouzon for providing the adiabatic effectiveness data for the $s = 1.0d$ trench configurations.

REFERENCES

[1] Bunker R., 2002, "Film Cooling Effectiveness due to Discrete Holes Within a Transverse Surface Slot" Paper No. GT-2002-30178, IGTI Turbo Expo, Amsterdam, Netherlands.

[2] Waye S. K., Bogard D.G., 2006, "High Resolution Film Cooling Effectiveness Measurements of Axial Holes Embedded in a Transverse Trench with Various Trench Configurations" Paper No. GT-2006-90226, IGTI Turbo Expo, Barcelona, Spain.

[3] Lu Y., Nasir H., Ekkad S.V., 2005, "Film Cooling from a Row of Holes Embedded in Transverse Slots" Paper No. GT-2005-68598, IGTI Turbo Expo, Reno-Tahoe, Nevada, USA.

[4] Dorrington, J.R. and Bogard, D.G., 2007, "Film Effectiveness Performance for Coolant Holes Embedded in Various Shallow Trench and Crater Depressions", ASME paper GT2007-27992.

[5] Ericksen, V. L. and Goldstein, R. J., 1974, "Heat Transfer and Film Cooling Following Injection Through Inclined Circular Tubes," ASME Journal of Heat Transfer , Vol. 107, pp. 239-245.

[6] Baldauf, S., Scheurlen, M., Schultz, A., Wittig, S., 2002, "Heat Flux Reduction From Film Cooling and Correlation of Heat Transfer Coefficients from Thermographic Measurements at Engine Like Conditions," ASME Paper No. GT-2002-30181.

[7] Ammari H., Hay, N., and Lampard, D., 1990. "The Effect of Density Ratio on the Heat Transfer Coefficient from a Film-Cooled Flat Plate," Journal of Turbomachinery, Vol. 112, pp. 444-450.

[8] Mayhew, J E., Baughn, J. W., and Byerley, A. R., 2002, "The Effect of Freestream Turbulence on Film Cooling Heat Transfer Coefficient," ASME Paper No. GT-2002-30173.

[9] Kelly. G. B., and Bogard, D. G., 2003, An Investigation of the Heat Transfer for Full Coverage Film Cooling," ASME Paper No. GT2003-3876.

[10] Coulthard, S. M., Volino, R. J., and Flack, K. A., 2006, "Effect of Unheated Starting Lengths on Film Cooling Effectiveness," ASME Journal of Turbomachinery, 128, pp. 579-588.

[11] Sen, B., Schmidt, D. L., Bogard, D. G., "Film Cooling with Compound Angle Holes: Heat Transfer," ASME Journal of Turbomachinery, 118, pp. 800-806.

[12] Robertson, D.R., 2004, "Roughness Impact on Turbine Vane Suction Side Film Cooling Effectiveness", MS Thesis, The University of Texas at Austin.

[13] Moffat, R.J., 1988, "Describing the Uncertainties in Experimental Results", *Experimental Thermal and Fluid Science*, Vol. 1, pp.3-17.